Respiratory Physiology & Neurobiology 194 (2014) 37–48

Contents lists available at ScienceDirect

Respiratory Physiology & Neurobiology

journal homepage: www.elsevier.com/locate/resphysiol

Low-level laser therapy inhibits bronchoconstriction, Th2 inflammation and airway remodeling in allergic asthma

Vanessa R. Silva[a], P. Marcondes[b], M. Silva[a], Antonio B. Villaverde[c], Hugo C. Castro-Faria-Neto[d], Rodolfo P. Vieira[a], Flavio Aimbire[b,*], Ana Paula L. de Oliveira[a]

[a] Nove de Julho University – UNINOVE, Laboratory of Pulmonary and Exercise Immunology – LABPEI, Rua Vergueiro 239/245, PO Box 01504-001, São Paulo, SP, Brazil
[b] Department of Science and Technology, Federal University of São Paulo, PO Box 12231-280, São José dos Campos, SP, Brazil
[c] Institute of Biomedical Engineering, Unicastelo, PO Box 12247-016, São José dos Campos, SP, Brazil
[d] Laboratory of Immunopharmacology, IOC, FIOCRUZ, PO Box 21045-900, Rio de Janeiro, RJ, Brazil

ARTICLE INFO

Article history:
Accepted 8 January 2014

Keywords:
Allergy
Airway hyperresponsiveness
RhoA
Eosinophils
STAT6
Laser therapy

ABSTRACT

Low-level laser therapy (LLLT) controls bronchial hyperresponsiveness (BHR) associated with increased RhoA expression as well as pro-inflammatory mediators associated with NF-kB in acute lung inflammation. Herein, we explore if LLLT can reduce both BHR and Th2 cytokines in allergic asthma. Mice were studied for bronchial reactivity and lung inflammation after antigen challenge. BHR was measured through dose–response curves to acetylcholine. Some animals were pretreated with a RhoA inhibitor before the antigen. LLLT (660 nm, 30 mW and 5.4 J) was applied on the skin over the right upper bronchus and two irradiation protocols were used. Reduction of BHR post LLLT coincided with lower RhoA expression in bronchial muscle as well as reduction in eosinophils and eotaxin. LLLT also diminished ICAM expression and Th2 cytokines as well as signal transducer and activator of transduction 6 (STAT6) levels in lungs from challenged mice. Our results demonstrated that LLLT reduced BHR via RhoA and lessened allergic lung inflammation via STAT6.

1. Introduction

Asthma is one of the most common diseases characterized by airway obstruction, airway inflammation and airway hyperresponsiveness (AHR) to a variety of stimuli (Burney, 1997). Current views propose airway inflammation as the underlying process, resulting in airway hyperresponsiveness and variable airflow obstruction. Cytokines have been increasingly recognized as playing an important role in the chronic inflammation response in asthma. Many inflammatory cells, mainly eosinophils, and structural cells, such as epithelial, smooth muscle, and endothelial cells, are capable of synthesizing and releasing these proteins (Barnes, 1999; Busse and Lemanske, 2001). Cytokines of particular importance for asthma include the lymphokines secreted by the T helper 2 (Th2)-type $CD4^+$ T lymphocytes. These cells produce and secrete interleukins IL-3, IL-4, IL-5, and IL-13. Moreover, IL-4 and IL-13 are essential for IgE switching of B lymphocytes, and the IL-5 selectively acts on eosinophil maturation, survival and activation. The presence of these cells and their products in the lung often correlate with disease severity and the degree of AHR (Azzawi et al., 1990; Broide et al., 1991; Ohashi et al., 1992).

The signal transducer and activator of transduction 6 (STAT6) is an essential transcription factor for IL-4 and IL-13 signaling. Using STAT-deficient mice, it was shown that STAT6 is essential for the induction of allergic asthma. Failure of these animals to develop allergic asthma has been considered to be due to a defect in IL-4- and/or IL-13-dependent Th2 differentiation and Ig class switching to IgE (Takeda et al., 1996; Kaplan et al., 1996; Emson et al., 1998). This finding reveals the importance of STAT6 for the initial phase induction of the Th2-dependent allergic response (Kuperman et al., 1998; Akimoto et al., 1998). Likewise, several research groups have reported that STAT6 also plays a critical role in the late phase of allergic asthma in mice. They demonstrated that airway hyperresponsiveness, IgE production and eosinophilia were fully dependent on STAT6 signaling in mice (Kuperman et al., 1998; Akimoto et al., 1998).

The AHR is an important symptom of disease, although the pathophysiological variations resulting in the hyperresponsiveness still remain unclear. Several mechanisms have been suggested to explain airway hyperresponsiveness, such as alterations in the

* Corresponding author at: Department of Science and Technology, Federal University of São Paulo – UNIFESP, Rua Talim, 330 – Vila Nair, PO Box 12231-280, São José dos Campos, SP, Brazil. Tel.: +55 12 3309 9578; fax: +55 12 3921 9512.
E-mail address: flavio.aimbire@unifesp.br (F. Aimbire).

1569-9048/$ – see front matter © 2014 Elsevier B.V. All rights reserved.
http://dx.doi.org/10.1016/j.resp.2014.01.008

neural control of airway smooth muscle (Boushey et al., 1980), increased mucosal secretions (Jeffery, 1993) and mechanical factors related to remodeling of the airways (Martin et al., 2000). In addition, it has also been suggested that one of the factors that contribute to the exaggerated airway narrowing in asthmatics is the abnormal nature of airway smooth muscle (Wiggs et al., 1990; Seow et al., 1998).

Smooth muscle contraction is mainly regulated by an increase in cytosolic Ca^{+2} concentrations in myocytes. Some studies have reported an additional mechanism, known as Ca^{+2} sensitization, in agonist-induced smooth muscle contraction, including airways (Chiba et al., 2001, 2003, 2005a,b). Although the detailed mechanism is not fully understood, there is increasing evidence that the monomeric GTP-binding protein RhoA and its downstream target, the Rho-kinase, are involved in the agonist-induced Ca^{+2} sensitization of airway smooth muscle contraction (Chiba et al., 2003). When the RhoA/Rho-kinase system is activated by contractile agonists, the activity of myosin light chain (MLC) phosphatase is reduced and the level of phosphorylated MLC in subsequently increased, resulting in an enhancement of smooth muscle contraction. It is possible that an increase in the RhoA/RhoA-kinase system is one of the causes for bronchial smooth muscle hyperresponsiveness. Furthermore, the importance of RhoA and its downstream RhoA-kinases on the contraction of human bronchial smooth muscle has also been proposed as a new target for the treatment of AHR in asthma (Gosens et al., 2006).

Low-level laser therapy (LLLT) has been used in experimental (Pires et al., 2011) and clinical (Chow et al., 2006) studies for the treatment of inflammatory diseases. It has been reported that LLLT can relieve the late and early symptoms of airway and lung inflammations by reducing the mRNA expression of inflammatory mediators, such as TNF-α and IL-1β (Aimbire et al., 2008; Mafra de Lima et al., 2009a,b). Moreover, LLLT reduces the cholinergic hyperreactivity and TNF-α mRNA expression in rat BSM segment exposure to lipopolysaccharide via a NF-kappaB-dependent mechanism (Mafra de Lima et al., 2009a,b). Our group has demonstrated that low-level laser irradiation is effectively beneficial in relieving airway hyperresponsiveness by reducing RhoA expression and the decrease in calcium sensitivity (Aimbire et al., 2009; de Lima et al., 2010). Thus, it would be relevant to determine whether LLLT can relieve bronchial hyperresponsiveness via a RhoA-dependent pathway, as well as to control lung inflammation via STAT6 signaling in animals with allergic asthma.

In this context, the present study was designed to investigate whether LLLT can modulate bronchial hyperresponsiveness to cholinergic stimulation and lung inflammation in a model of allergic asthma in rat.

2. Materials and methods

2.1. Animals

All experiments were performed according to the guidelines of Vale do Paraíba University (Univap) for animal care (A06/CEP/2008). The assays were performed on eight-week-old male BALB/c mice, which were maintained under standard conditions of temperature (22–25 °C), relative humidity (40–60%) and light/dark cycle with access to food and water ad libitum.

2.2. Anesthesia

The animals were pre-anesthetized with Acepromazine (0.1 mg kg^{-1}) and anesthetized with Zolazepam Chloride (2.5 mg kg^{-1}) + Tiletamine Chloride (2.5 mg kg^{-1}). For euthanasia, the mice received an excessive dose of chloral hydrate (>400 mg kg^{-1}, i.p.) under anesthesia.

2.3. Sensitization and antigen challenge

Mice were sensitized via an intraperitoneal injection of a suspension of 10 μg of ovalbumin (OVA) with 10 mg aluminum hydroxide. One week later, the rats were boosted subcutaneously with 10 μg of OVA dissolved in phosphate buffer solution (PBS). Two weeks after the first sensitization, the mice were subjected to a single 15-min exposure to aerosolized OVA (1% in PBS) using an ultrasonic nebulizer device (ICEL, São Paulo, Brazil) coupled to a plastic inhalation 7 chamber (18.5 cm × 18.5 cm × 13.5 cm). The mice were euthanized 24 h after challenge by sectioning the abdominal aorta under deep chloral hydrate anesthesia (>400 mg kg^{-1}, i.p.), and then the measurements were performed.

2.4. Low-level laser therapy (LLLT)

Animals challenged with OVA were irradiated using a CW laser diode module (MM Optics, São Paulo, Brazil) with the following parameters: output power of 30 mW, 660 nm wavelength, spot size of 0.08 cm^2, resulting in an optical power density of 375 mW cm^{-2}. The optical power was calibrated using a Newport 1835 C multifunction optical power meter (Equipland, Oklahoma Road, Sao Jose, CA, USA). The laser power was monitored during laser irradiation by collecting laser light with a partial reflection (4%) mirror. The laser irradiation dose was set at 5.4 J for 3 min. Two series of laser irradiation protocols were performed: Protocol I – the mice were divided into four different groups, where each mouse received a unique irradiation dose of low-level laser at 5 min, 1 h, 6 h or 12 h after antigenic response, respectively; Protocol II – all mice from one group were irradiated on the skin over the right upper bronchus at four consecutive times 5 min, 1 h, 6 h and 12 h from the antigen challenge. Twenty-four hours after the antigenic challenge, the bronchial reactivity, RhoA mRNA expression in BSM, IgE level in sera and lung inflammation were analyzed.

2.5. Experimental groups

The animals were provided by the Central Animal House of the University of São Paulo – USP. All mice were placed in a common box and divided randomly into nine groups consisting of seven animals: (1) *control* group, which consisted of non-manipulated mice; (2) *laser* group, where animals were non-challenged and treated with laser irradiation; (3) the *challenged* group, which consisted of mice subjected to antigen exposure, without treatment; (4) animals that received inhalation of Y-27632 for 3 min, 1 h prior to the antigenic challenge; (5–8) challenged + laser groups (I): sensitized and challenged mice, which were treated with laser once for 3 min at the following irradiation times after the antigenic challenge: at 6 min, 1 h, 6 h, or 12 h, respectively (irradiation protocol I) and (9) the *challenged + laser* group (II), sensitized and challenged animals, treated with laser for 3 min, and then at four consecutive times: 6 min, 1 h, 6 h and 12 h after antigenic challenge (irradiation protocol II). Table 1 summarizes the experimental groups.

2.6. Pharmacological intervention

As a positive control for the contribution of RhoA in the hyperresponsiveness of BSM, the mice received inhalation of Y-27632 (Chiba et al., 2005b) (RhoA inhibitor 10 μM; Tocris Cookson, Bristol, UK) for 3 min, 1 h prior to the antigenic challenge. Twenty-four hours after antigenic exposure, BSM segments from mice were

Table 1
Description of the experimental groups.

Group	Description
(1) Control	Non-sensitized and non-challenged animals
(2) Laser	Non-sensitized animals, treated with laser for 3 min at the four consecutive times: 5 min, 1 h, 6 h and 12 h after antigenic challenge (irradiation protocol II)
(3) Challenged	Sensitized and challenged animals
(4) Y-27632 + challenged	Animals received inhalation of Y-27632 for 3 min, 1 h before the antigenic challenge
(5–8) Challenged + laser (I)	Sensitized and challenged animals, treated with laser once for 3 min at the following irradiation times after antigenic challenge (irradiation protocol I) 5 min 1 h 6 h 12 h
(9) Challenged + laser (II)	Sensitized and challenged animals, treated with laser for 3 min, at the four consecutive times: 5 min, 1 h, 6 h and 12 h after antigenic challenge (irradiation protocol II)

prepared for functional studies of contractility, and RhoA mRNA expression analyses.

2.7. Preparation of bronchial smooth muscle (BSM) and functional study

To determine the change in bronchial smooth muscle contractility, the isometric contraction of the circular smooth muscle of the main bronchus was measure as previously reported (Aimbire et al., 2009). Briefly, 24 h after the last antigen challenged, the mice were sacrificed under anesthesia. After thoracotomy, blood samples were collected from the hearts to obtain sera, and bronchoalveolar lavage (BAL) was performed as previously described (Aimbire et al., 2009). The airway tissues from the larynx up to the lungs were then immediately removed. The left main bronchus was isolated and then suspended in an organ bath at a resting tension of 1 g. The organ bath contained modified Krebs–Henseleit solution consisting of (mM): 118.0 NaCl, 4.7 KCl, 2.5 $CaCl_2$, 1.2 $MgSO_4$, 25.0 $NaHCO_3$, 1.2 KH_2PO_4 and 10.0 glucose (pH 7.4). The isometric contraction of the circular smooth muscle was measured using a force-displacement transducer (MP100, BioPac, CA, USA). The tissues were washed three or four times at time intervals of 15–20 min, and then slowly equilibrated to a baseline tension of 0.5 g. After the equilibration period, the concentration–response curve to acetylcholine (ACh: 10^{-7}–10^{-3} M final concentration) was cumulatively constructed. In another series of experiments, isotonic K^+ solution (10–60 mM final concentration) was cumulatively administered in the presence of atropine and indomethacin (both 10^{-6} M) to determine the bronchial smooth muscle responsiveness to high-K^+ depolarization (Table 2).

2.8. Quantification of bronchoalveolar lavage fluid (BALF) cellularity

Twenty-four hours after antigenic challenge, the animals were euthanized under anesthesia and the trachea was cannulated. BALF cells were collected from the airway lumen by flushing the airways with a 10 mg kg^{-1} RPMI 1640 through the tracheal cannula. This procedure was repeated and a pool of samples for each animal was obtained. The samples were refrigerated for subsequent use. Total cell counts were obtained in the BALF samples using an automated cell counter (Sellex, USA). The cytospins of these samples were prepared by centrifugation of 100 μL aliquots in a cytospin (Sellex, USA) at 700 rpm for 5 min at low acceleration and room temperature. The slides were fixed and stained using a Hema-tek 2000 (BioRad, USA) with Wright–Giemsa stain. The cells were quantified according to the standard morphological criteria. The BALF cellularity data were expressed as cells mL^{-1}.

2.9. Histology and histomorphometric analysis of inflammation, collagen and mucus

2.9.1. Histology and image analysis

Five micrometer slides were stained with hematoxylin and eosin, picrossirius, and periodic acid Shiff and Alcian blue to identify and quantify the density of the eosinophils in the airway walls, the density of collagen fibers in the airway walls and the neutral and acid mucus in the airway epithelium, respectively. Five airways of all animals were imaged at 400× magnification using a Nikon Eclipse E-200 microscope, a camera infinity and the software Image Pro-Plus 4.0. The color threshold for collagen, periodic acid Shiff (PAS) and Alcian blue (AB) were determined and the analyses were performed as follows:

2.9.2. Eosinophil density in airway wall

The area between the airway basal membrane and the adventitia was quantified using the software Image Pro-Plus and the number of eosinophils was quantified in this area according to the morphological criteria. These results were expressed as the number of eosinophils per square millimeter.

2.9.3. Percentage of neutral and acid mucus

The airway epithelium area was determined. Next, using the previously determined color threshold for neutral mucus (PAS positive) and for acid mucus (AB positive), the amount of PAS and AB area was determined. These results were expressed as the % of PAS and AB area compared to the total epithelium.

2.9.4. Percentage of collagen fibers deposition in the airway wall

First, the area between the airway basal membrane until the airway adventitia was determined. Next, using the previously determined color threshold for picrossirius and the picrossirius-positive area was quantified. These results were expressed as the % of collagen (picrossirius positive) area compared to the total measured area.

2.9.5. Peribronchial edema

To measure the amount of peribronchial edema, transversely sectioned noncartilaginous airways were selected and magnified 1000×. The number of points of the interacting eyepiece falling on areas of edema was quantified in three randomly selected areas of each airway wall.

2.9.6. Index of bronchoconstriction

The airway bronchoconstriction index was assessed as the number of points hitting the airway lumen divided by the root square of the number of intercepts between the lines of the grid and the airway basal membrane. Measurements were performed in five airways from each animal at 400× magnification.

Table 2
Description of the histology.

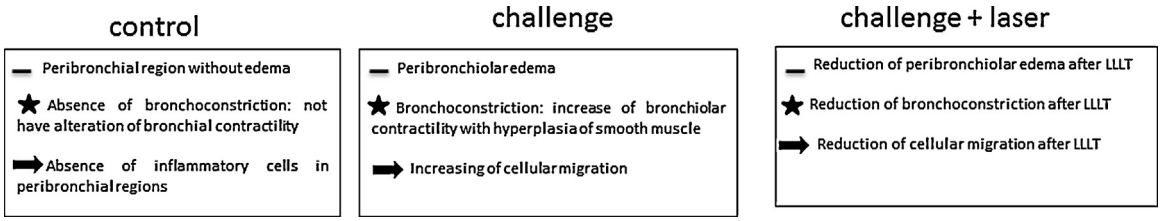

2.10. Immunohistochemical of ICAM-1 in lung

Paraffin sections of lung tissue were processed for standard immunohistological staining using the labeled streptavidin-biotin method and polyclonal rabbit anti-mice ICAM-1 antibody diluted at 1:100 (Santa Cruz Biotechnology, Santa Cruz, CA, USA). The secondary antibody consisted of biotinylated sheep anti-rabbit immunoglobulin (Santa Cruz Biotechnology, Santa Cruz, CA, USA) containing 10% normal rat serum. The tertiary antibody was streptavidin–horseradish peroxidases conjugated antibodies (Santa Cruz Biotechnology, Santa Cruz, CA, USA). The positive reaction was visualized as a brown stain following treatment with 3,3-diaminobenzidine. Sections were counterstained with Mayer's hematoxylin solution. Immunohistochemical images (five images from each sample collected from all mice in each experimental group) were assessed using the Imaging Densitometer (AxioVision, Zeiss, USA) and a computer program (AxioVision).

2.11. Real time-PCR for RhoA and ICAM-1 mRNA expression

Twenty-four hours after the antigenic challenge, the thoracic cavity of the mice was exposed and the heart and lung were removed in bloc. The pulmonary artery was cannulated and then the pulmonary vasculature was perfused with ice-cold sterile phosphate buffer solution (PBS) using a peristaltic pump (Thermo Fisher Scientific, Suwannee, GA) to remove the intravascular blood. BSM segments (RhoA mRNA expression) or lung fragments (ICAM-1 mRNA expression) were cut into 5-mm pieces using a tissue chopper, flash-frozen in liquid nitrogen and stored at −80 °C for Real Time-PCR (RT-PCR) analysis of gene expression. Next, total RNA was isolated from lung using TRIzol reagent (GibcoBRL, Gaithersburg, MD), according to the manufacturer's protocol. RNA was subjected to DNase I digestion, followed by reverse transcription to cDNA, as previously described by Cayla and colleagues (Cayla et al., 2002). PCR was performed in a 7000 Sequence Detection System (ABI Prism, Applied Biosystems, Foster City, CA) using the SYBRGreencore reaction kit (Applied Biosystems). Primers used for RhoA and ICAM-1 mRNA quantification were mouse RhoA 195–305 (GenBank™accession number X66539) forward primer 5′-CTGGTTGGGAACAAGAAGGA-3′ and reverse primer 5′-CAAAAACCTCCCTCACTCCA-3′; mouse Exon (GenBank™accession number D00475), ICAM-1 793–871 (GenBank™ accession numberM98820) forward primer 5′-CACCTCTCAAGCAGAGCACAG-3′ and reverse primer 5′-GGGTTCCATGGTGAAGTCAAC-3′; mouse Exon (GenBank™ accession number NW047658) and mouse β-actin-3474–3570 (GenBank™ accession number J00691) forward primer 5′-TTCAACGGCACAGTCAAGG-3′ and reverse primer 5′-ACATACTCAGCACCAGCATCAC-3′ were used as control. The quantitative values for RhoA and β-actin mRNA transcription were obtained from the threshold cycle number, where an increase in the signal growth of PCR products could be detected. Melting curves were generated at the end of every run to ensure product uniformity. The relative target gene expression level was normalized on the basis of β-actin expression as endogenous RNA control. The ΔC_t values of the samples were determined by subtracting the average C_t value of RhoA mRNA from the average C_t value of the internal control β-actin. Because it is uncommon to use ΔC_t as a relative data due to the logarithmic characteristic, the $2^{-\Delta C_t}$ parameter was used to express the relative expression data (Livak et al., 1999). These results are expressed as the ratio relative to the sum of β-actin transcript level as an internal control.

2.12. Lung tissue sampling and processing mediators

After BALF was performed, the thoracic cavity was exposed and the heart and lung were removed in bloc. The two major lung lobes were dissected and the pulmonary vasculature of the lobes was perfused with ice-cold sterile phosphate buffer solution (PBS) using a peristaltic pump (Sellex, USA) to remove the blood poll of cells. Next, the lobes were cut into 5-mm pieces using a tissue chopper, flash-frozen in liquid nitrogen and stored at −80 °C for further analyses using an enzyme-linked immunosorbent assay (ELISA) of inflammatory protein.

2.13. BALF cytokines and Lung ICAM-1

The pro-inflammatory mediator levels in BALF were determined using the Enzyme Linked Immuno Sorbent Assay (ELISA) with commercially available kits according to the manufacturer's instructions. Interleukins-4, -5, -13 and eotaxin concentrations were determined using a solid phase sandwich ELISA kit, using peroxidase and tetramethylbenzidine as a detection method (Bio-Rad, USA). The detection limit of these assays was within the range of 1–5 pg mL^{-1}. For lung tissue, ICAM-1 levels were further corrected for protein content using the Lowry assay. The protein data in BALF and lung tissue were expressed as ng mL^{-1} and pg mg^{-1}, respectively.

2.14. Quantification STAT6 protein in lung

STAT6 in lung tissue was determined using the ELISA kit, which quantifies this transcription factor independently of phosphorylation status and enables normalization of phosphorylated STAT6 to total STAT6. Briefly, the STAT6 antigen binds to the immobilized (capture) antibody during the first incubation. After washing, a rabbit antibody specific for STAT6 phosphorylated at tyrosine 641 is added to the wells. During the second incubation, this antibody serves as a detection antibody by binding to the immobilized STAT6 protein, which was captured during the first incubation. After removal of the excess detection antibody, a horseradish peroxidase-labeled anti-rabbit IgG (anti-rabbit IgG-HRP) is added. This binds to the detection antibody to complete the four-member sandwich. After the third incubation and washing to remove all the excess of anti-rabbit IgG-HRP, a substrate solution is added, which is activated by the bound enzyme to produce a color precipitate. The intensity of this colored product is analyzed using a spectrophotometer (450 nm) and is directly proportional to the concentration of STAT6 present in the lung tissue. The analytical sensitivity of this assay is <1.25 units mL^{-1} of STAT6.

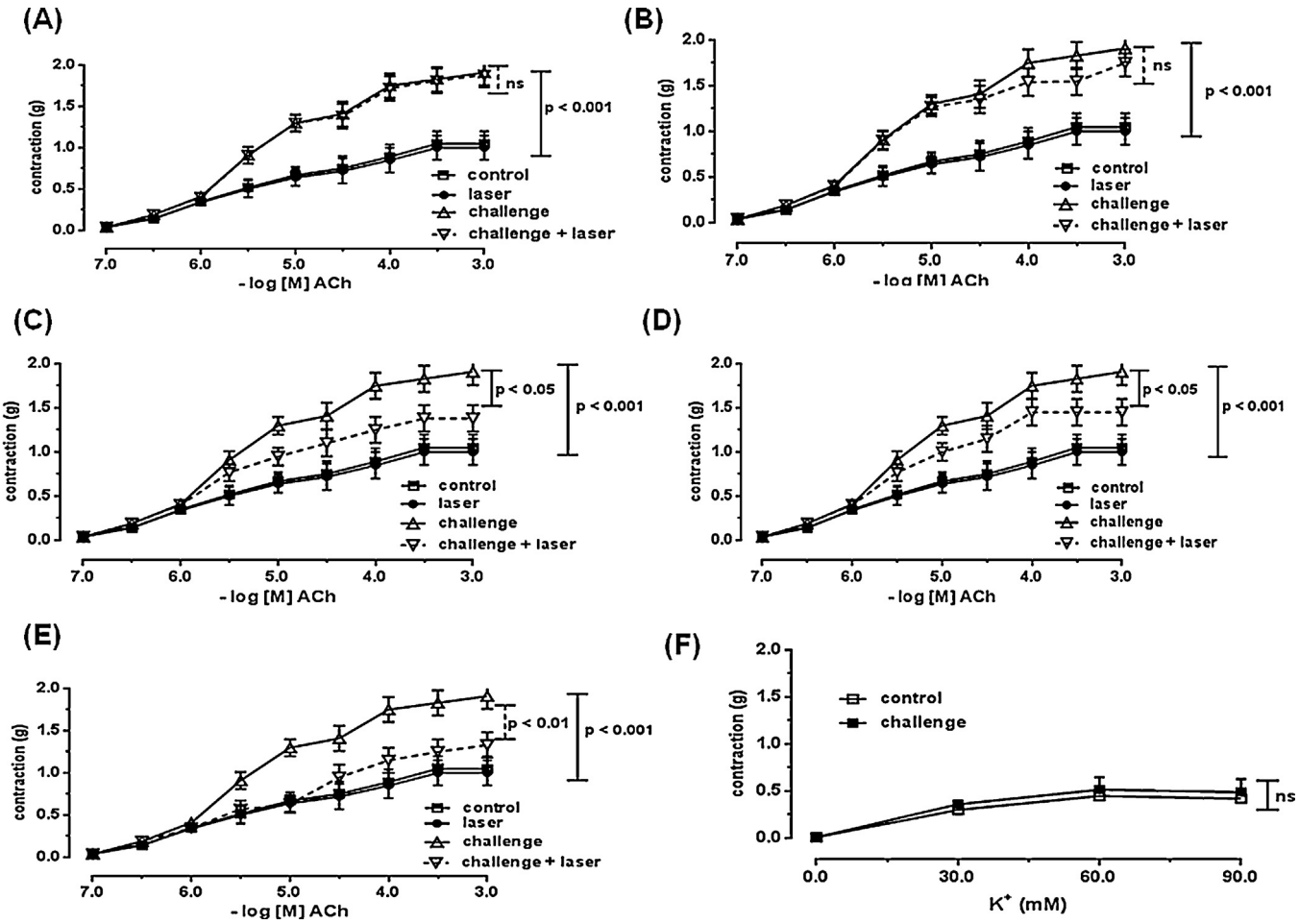

Fig. 1. Effect of LLLT on the bronchial smooth muscle hyperresponsiveness. ACh-induced depolarization/contractions of bronchial smooth muscles were measured isometrically in control, laser, antigen challenged and antigen challenged + laser groups (A–E). The animals were treated with one dose of laser irradiation for 3 min on the skin over the upper bronchus at 5 min (A), 1 h (B), 6 h (1 C) and 12 h (D), after antigen challenge (irradiation protocol I). (E) illustrates the bronchial hyperresponsiveness of animals treated with 4 consecutive doses of laser at times of 5 min, 1, 6 and 12 h after antigenic response (irradiation protocol II). (F) represents the high-K^+ depolarization-induced contractions of bronchial smooth muscles of animals from control and challenged groups. The bronchial smooth muscle reactivity to acetylcholine was measured 24 h after antigen challenge in all experiments. Each point represents mean ± SE from 7 different animals.

2.15. Quantification of IgE level in serum

Serum was obtained from the blood sample by centrifugation at 3000 × *g* for 10 min at 4 °C. The total IgE in serum was measured using enzyme-linked immunosorbent assay (ELISA) with a Rat IgE ELISA kit (Invitrogen, SP, Brazil) according to the manufacturer's instructions.

2.16. Statistical analysis

Significant differences were evaluated using analysis of variance (ANOVA) and Tukey–Kramer Multiple Comparisons Test to determine the differences between groups. These results were considered significant when $p < 0.05$.

3. Results

3.1. Effect of LLLT on bronchial smooth muscle hyperresponsiveness

The ACh responsiveness of bronchial smooth muscles isolated from non-sensitized and antigen-challenged rats is shown in Fig. 1. The non-sensitized animals were used as controls. Application of ACh (10^{-7}–10^{-3} M) to isolated bronchial smooth muscles elicited a concentration-dependent contraction in all animals studied. The contractile response to ACh of bronchial smooth muscle from the antigen-challenged rats was markedly enhanced when compared with control animals: the ACh concentration-response curve was significantly shifted upward by the antigen exposure. However, non-significant changes in the contractile response induced by high-K^+ depolarization were observed between groups (Fig. 1F). The effect of LLLT on the bronchial smooth muscle responsiveness can be observed from Fig. 1A–E. The contractile response to ACh in the group animals irradiated only once at 5 min (1A), 1 h (1B), 6 h (1C) or 12 h (1D) after last antigen inhalation (irradiation protocol I) are shown in Fig. 1A–D; whereas Fig. 1E represents the response of the animals irradiated at four consecutive times (irradiation protocol II). Furthermore, laser irradiation had no effect on the animals in the control group at any time studied. However, the increase of the ACh-induced contraction, i.e., bronchial smooth muscle hyperresponsiveness, which was observed in the antigen-challenged rats, was significantly inhibited by the LLLT for both laser irradiation protocols, with the exception of the irradiations at the early times of 5 min and 1 h after antigenic challenge (Fig. 1A and B).

3.2. Effect of Y-27632 on bronchial smooth muscle hyperresponsiveness

To confirm the involvement of RhoA system in bronchial hyperresponsiveness observed in the antigen-challenged rats, the

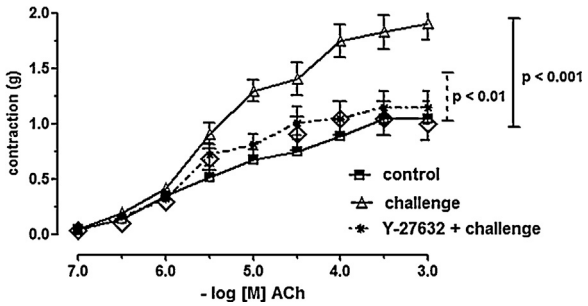

Fig. 2. Effect of RhoA inhibitor on bronchial hyperresponsiveness. To confirm the RhoA participation in bronchial hyperresponsiveness in antigen challenged mice, animals were treated with RhoA inhibitor, Y-27632 (10 μM) 1 h before antigen challenge. Bronchial smooth muscles obtained from animals not challenged were used as control. The bronchial smooth muscle hyperresponsiveness to acetylcholine was measured 24 h after antigen challenge. Each bar represents mean ± SE from 7 different animals.

animals were treated with Y-27632, a RhoA inhibitor, by inhalation 1 h prior to the antigenic challenge (Fig. 2). After treatment of Y-27632, the bronchial hyperresponsiveness to ACh completely returned to control levels. In addition, the RhoA inhibitor had no effect on the contractility of bronchial smooth muscle to ACh in control animals.

3.3. Effect of LLLT or Y-27632 on RhoA mRNA expression

The levels of total RhoA mRNA expression from all animal groups are shown in Fig. 3: animals that were challenged or not challenged and laser-treated or non-treated, were examined for mRNA expression of the main and intrapulmonary bronchial smooth muscles in the absence of epithelia and lung parenchyma. The RhoA mRNA expression in bronchial smooth muscle of the antigen-challenged rat was significantly increased compared to the control group. The laser treatment had no effect on the RhoA expression in the control group. However, LLLT markedly blocked the upregulation of RhoA expression in BSM from antigen-challenged rats. Moreover, an enhanced inhibitory effect on expression was obtained when the rats subjected to antigenic challenge were initially treated with the Y-27632 RhoA inhibitor. This inhibitor decreases RhoA mRNA expression in BSM segments from allergic rats to control levels. The RhoA inhibitor had not effect on RhoA mRNA expression in BSM segments from the control and laser-treated groups.

3.4. Effect of LLLT on allergic inflammation in the lung and IgE levels in serum

To determine the effect of LLLT on changes in airway biology induced by antigen exposure, the total cell number in BAL was quantified and histological analysis was performed. We found that the total number of cells in BAL of antigen-challenged rats was significantly increased when compared with the control group (Fig. 4A). Moreover, this increase was significantly reduced by LLLT. Diff-Quik cell staining revealed that most of the new cells were eosinophils and that the number of eosinophils in BAL from the antigen-challenged mice was largely reduced by LLLT (Fig. 4B). Histological examinations also revealed increased eosinophilic inflammation in the airway walls of antigen-challenged mice compared with the control group (Fig. 4C). Furthermore, laser treatment reduced eosinophilic inflammation induced by antigenic challenge compared with antigen-challenged mice, but not in treated mice (Fig. 4C and D). Histological alterations in lung parenchyma and peribronchiolar region were also characterized by the appearance of peribronchial edema and bronchoconstriction with metaplasia of bronchiolar smooth muscle cells (Fig. 4E and F). The levels of total IgE in sera of rats are shown in Fig. 4G. A marked increase in total IgE levels in animals that were sensitized and challenged with antigen was observed and this increase was not altered when these animals were laser-treated. Moreover, laser irradiation of the control group showed no effect on the total levels of IgE.

3.5. Effect of LLLT on ICAM-1

The LLLT effect on ICAM-1 mRNA (5A) and protein (5B) expression is shown in Fig. 5. Lung localization of ICAM-1 was marked with immunohistochemical staining (5C). Both ICAM-1 mRNA and protein expression in the lung was significantly higher in the challenge group compared with the control group (Fig. 5A and B, respectively); however, there was a significant decrease in ICAM-1 expression and protein in lungs harvested from animals treated with laser irradiation (Fig. 5A and B). The presence of ICAM-1 in lungs from challenged animals is confirmed by immunohistochemical staining in Fig. 5C and is also evidenced by the low-level laser therapy effect directly on ICAM-1. Laser irradiation on animals from the control group showed no effect on ICAM-1 expression.

3.6. Effect of LLLT on the deposition of mucus and collagen

These results demonstrated that OVA sensitization and LLLT treatment significantly increased and decreased neutral and acid mucus production, respectively (Fig. 6A and B, respectively). An increase in secretion in the lungs of challenged mice and the low-level laser therapy effect directly on mucus are shown in Fig. 6C. Moreover, OVA sensitization significantly increased secretion as well as the deposition of collagen in the airway wall, while LLLT significantly reduced the production and deposition of collagen (Fig. 7A and B, respectively).

3.7. Effect of LLLT on IL-4, IL-5, IL-13 and eotaxin

As shown in Fig. 8, the levels of IL-4 (8A), IL-5 (8B), IL-13 (8C) and eotaxin (8D) in BAL fluids of antigen-challenged rats were significantly increased compared with those from the non-sensitized animals (control group). The LLLT of animals from control group had no effect on the levels of these parameters. However, the levels of IL-4 and IL-5 in BAL from the antigen-challenge rats were reduced after laser therapy when compared with animals challenged, but not treated with laser, where the levels remained higher than the control group. In addition, LLLT markedly reduced both the IL-13 and eotaxin levels in BAL in the antigen-challenged rats compared with those in the laser-untreated animals. No significant differences were observed between the control and laser groups.

3.8. Effect of LLLT on STAT6

There was a significant change in the STAT6 protein levels in the challenge group compared with the control group, where the levels were strongly reduced when the animals were treated with laser (Fig. 9). Moreover, laser irradiation on animals not challenged with antigen (control group) had no effect on the level of STAT6 protein in lung tissue.

4. Discussion

Currently, available therapies for asthma are non-curative. These treatments only control inflammation, without altering the underlying immune reactivity, which predisposes the individual to atopic airway inflammation (Virchow and Barnes, 2012). Inhaled glucocorticoids are currently the mainstay of asthma therapy. Although this treatment is generally effective and well tolerated,

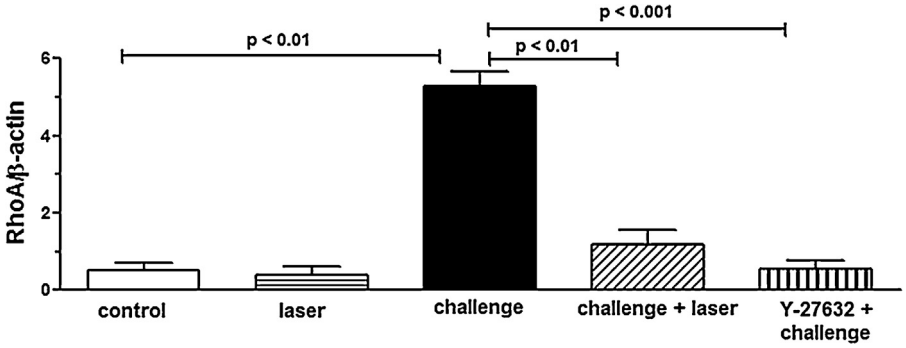

Fig. 3. Effect of RhoA inhibitor on upregulation of RhoA mRNA in bronchial smooth muscles. Bronchial smooth muscles obtained from control and antigen challenged mice were assayed for RhoA mRNA expression by Real Time-PCR technique. The animals were treated with laser for 3 min on skin over the upper bronchus at 5 min, 1, 6 and 12 h after antigen challenge or RhoA inhibitor, Y-27632 (10 μM) 1 h before the antigenic challenge. The PCR primer efficiencies were calculated using standard curves 24 h after allergic challenge. Each bar represents mean ± SE from 7 different animals.

several side effects, such as an impairment of growth, abnormalities in the metabolism of glucose, adrenal suppression, increased risk of fracture and the formation of cataracts may occur when they are used at high doses or for an extended period of time. Topical adverse effects, such as candidiasis and dysphonia have also been previously described with inhaled glucocorticoids. Sometimes resistance to glucocorticoids treatment occurs due to the usually higher dose requirements of glucocorticoids in these patients, which results in an increased risk of systemic side effects (Louis et al., 2012). For these patients, there is an urgent need to develop new anti-inflammatory therapies with immunomodulatory activity to provide alternative strategies to treat asthma.

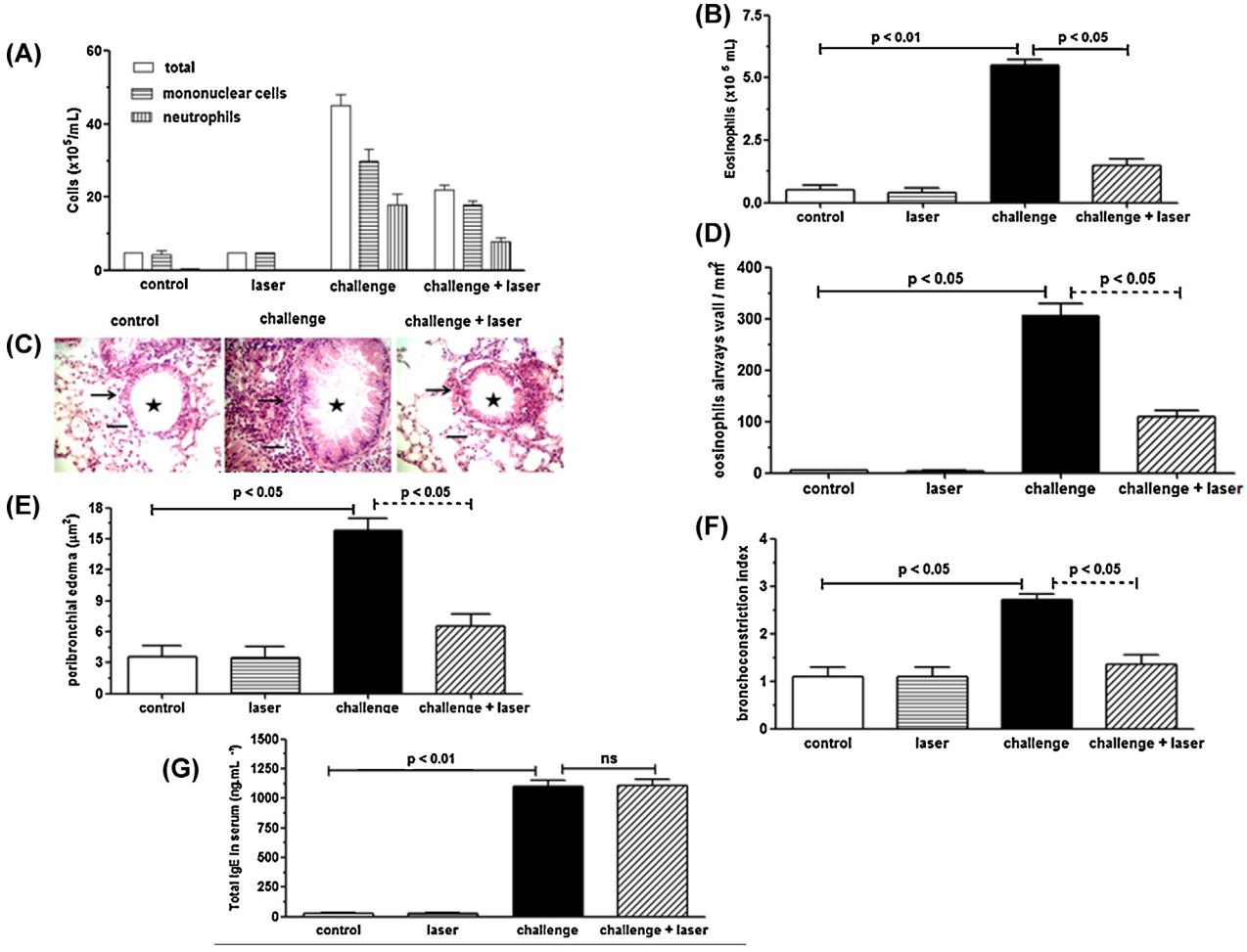

Fig. 4. Effect of LLLT on lung inflammation and on levels of total immunoglobulin E (IgE) in serum. Total, mononuclear and neutrophil cells count (Fig. 4A) and eosinophils (Fig. 4B) were carried out in BALF obtained from all studied groups. Sections (5 μm) of formalin-fixed lungs were stained with hematoxylin and eosin for histological examination (C) aiming to identify and quantify the density of eosinophils in airways wall (D) (original magnification, ×200). Bronchoconstriction index (E) and the percentage of peribronchiolar edema (F) were measured as described in Material and Methods section. Blood serum obtained from all mice was assayed for IgE by using enzyme-linked immunosorbent assay (ELISA). The IgE levels in serum were measured 24 h after the antigen challenge (G). The animals were treated with laser on skin over the upper bronchus at 5 min, 1, 6 and 12 h after antigen challenge. Each bar represents mean ± SE from 7 different animals.

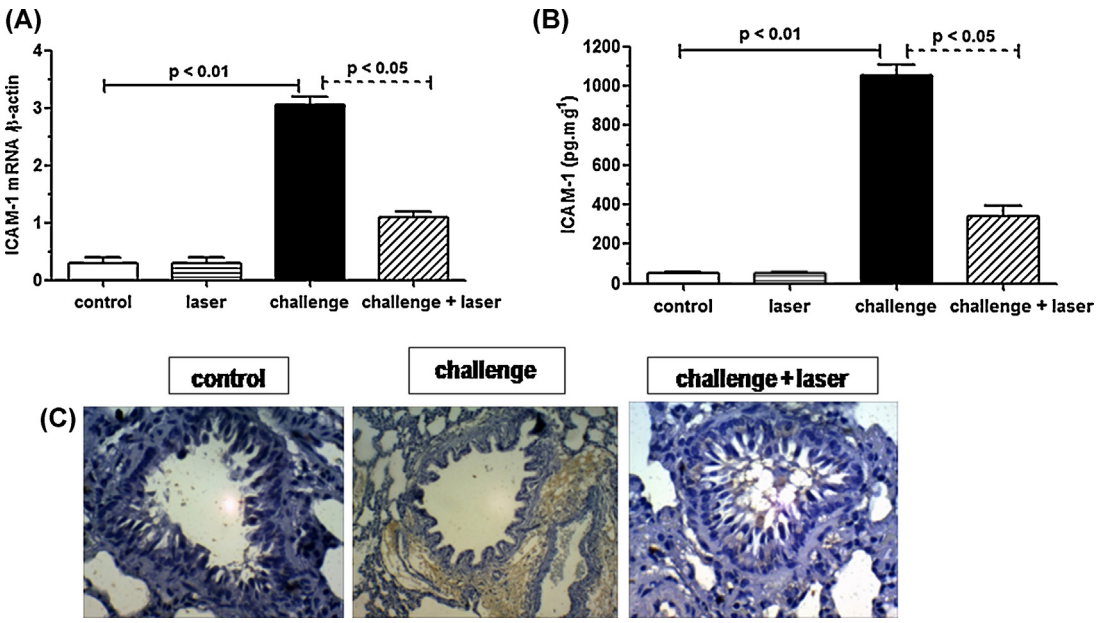

Fig. 5. Effect of LLLT on ICAM-1 protein expression in lung. The changes in ICAM-1 expression for all groups, control, laser, antigen challenge and antigen challenged + laser, are illustrated in the figure. The changes in ICAM-1 expression were assessed by mRNA expression (A) and by protein concentration by ELISA (B). For immunohistochemical localization of ICAM-1 in lung, the positive reaction was visualized as a brown stain (C). The animals were treated with laser on skin over the upper bronchus at 5 min, 1, 6 and 12 h after antigen challenge. Each bar represents mean ± SE from 7 different animals.

Since 1967, over 100 phase III, randomized, double-blind, placebo-controlled, clinical trials (RCTs) with low-level laser irradiation have been published and supported by more than 1000 laboratory studies investigating the primary mechanism and the signaling cascade of secondary effects that contribute to the arrangement of local tissue, as well as the systemic effects of laser treatment. RCTs with positive outcomes have been published on pathologies as diverse as osteoarthritis (Bjordal et al., 2006), back pain (Chow et al., 2009), stroke (Lampl et al., 2007) and pulmonary disorders, such as chronic obstructive bronchitis and asthma (Nedeljković et al., 2008; Kashanskaia and Fedorov, 2009). Nevertheless, these results have not been always been positive. This failure can be attributed to several factors, such as dosimetry (too low or too much energy delivered, too low or too much irradiance, inappropriate pulse structure, irradiation of insufficient area of the pathology), inappropriate anatomical treatment location and concurrent patient medication (such as steroidal and non-steroidal anti-inflammatory which can inhibit healing) (Huang et al., 2009). Due to the many existing physical parameters, which can directly affect the laser activity and its beneficial anti-inflammatory effects on diverse diseases, we performed a series of experimental studies within the last 6 years in order

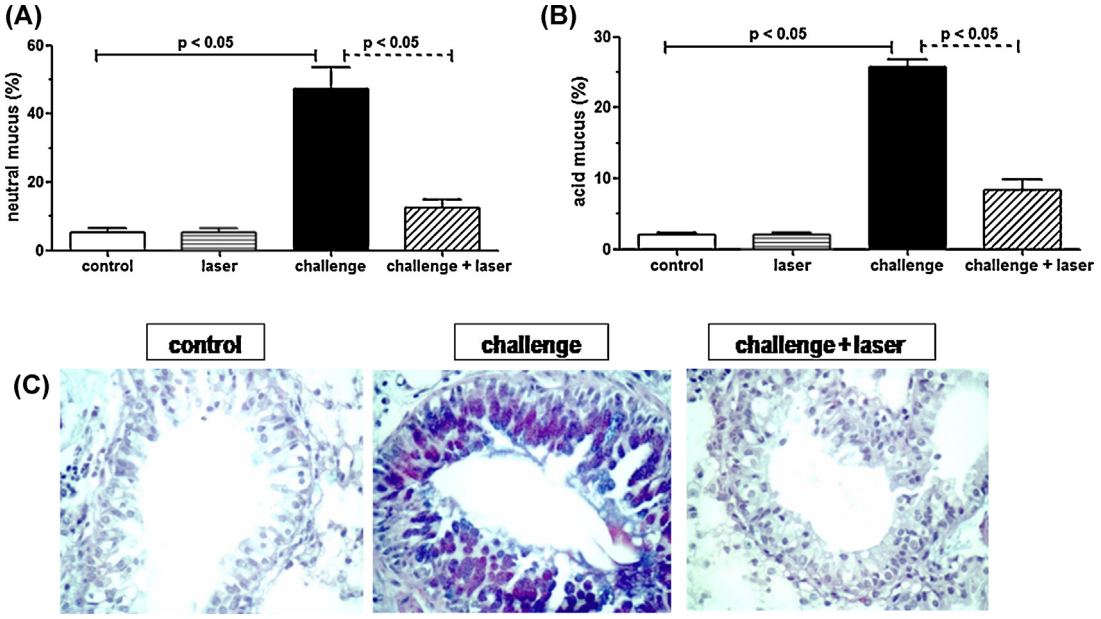

Fig. 6. Effect of LLLT on mucus production in lung. Sections of formalin-fixed lungs were stained with Periodic Acid Schif (PAS) before histological examination using light microscopy (original magnification, ×200). The animals were treated with laser on skin over the upper bronchus at 5 min, 1, 6 and 12 h after antigen challenge. Each bar represents mean ± SE from 7 different animals.

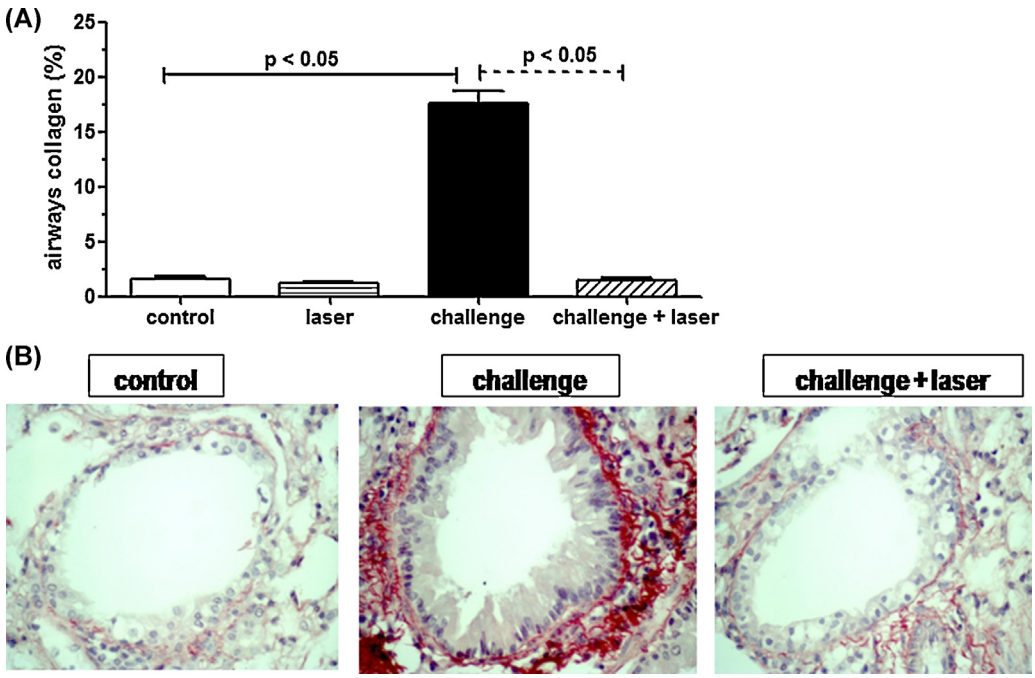

Fig. 7. Effect of LLLT on collagen production in lung. Sections of formalin-fixed lungs were stained with Picrossirius before examination with light microscopy (original magnification, ×200). The animals were treated with laser on skin over the upper bronchus at 5 min, 1, 6 and 12 h after antigen challenge. Each bar represents mean ± SE from 7 different animals.

to clarify which of the inflammatory mediators is the target for LLLT in pulmonary disorders, thereby initiating an understanding of the cellular signaling pathways responsible for the laser anti-inflammatory effect in inflammatory conditions, which compromise the lung and airway.

In clinical practice, the beneficial effects of LLLT have been demonstrated in patients with compromised airway and lung, particularly asthmatics (Esaulenko et al., 2009; Nikitin et al., 2008; Nedeljković et al., 2008; Farkhudtinov, 2007). In fact, several studies have demonstrated that LLLT provides a significant improvement in the course of bronchial asthma, enabling for outpatient treatment and rehabilitation, recovery of bronchial sensitivity to sympathomimetics and xanthine derivatives, lower glucocorticoid doses, shorter hospital stays, and reduced bronchial asthma-related disability (Nikitin et al., 2008; Ostronosova, 2006; Milojevic and Kuruc, 2003; Landyshev et al., 2002). Thus, additional studies are needed

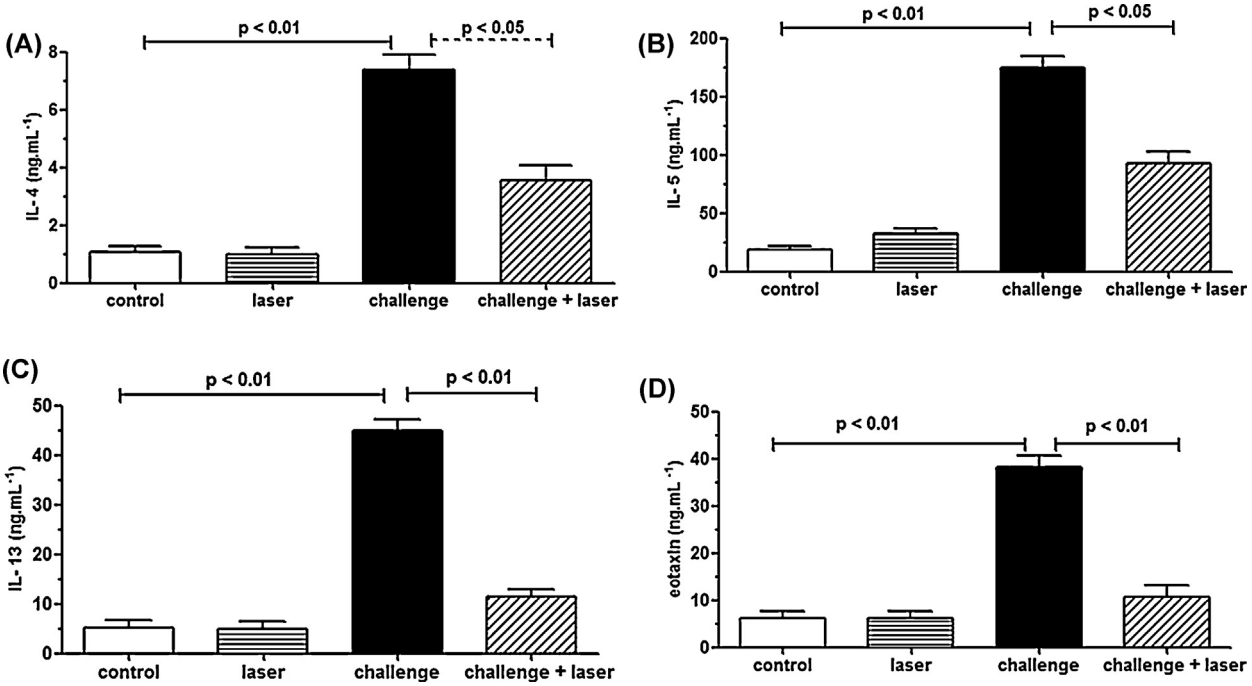

Fig. 8. Effect of LLLT on cytokines levels in BALF. BALF obtained from control, laser, antigen challenge and antigen challenged + laser groups were assayed for IL-4 (A), IL-5 (B), IL-13 (C) and eotaxin (D) by enzyme-linked immunosorbent assay (ELISA). The animals were treated with laser on skin over the upper bronchus at 5 min, 1, 6 and 12 h after antigen challenge. The cytokines levels in BALF were assayed 24 h after the antigen. Each bar represents mean ± SE from 7 different animals.

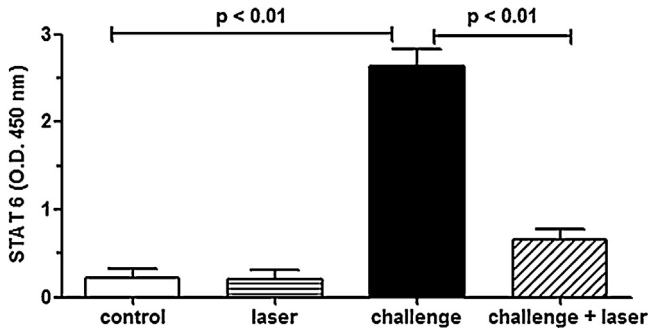

Fig. 9. Effect of LLLT on signal transducer and activator of transduction 6 (STAT6) in lung. The STAT6 concentration in lung tissue from control, laser, antigen challenge and antigen challenged + laser groups was determined by ELISA. The intensity of colored product analyzed in 450 nm is directly proportional to the concentration of STAT6 present in the lung tissue. The animals were treated with laser on skin over the upper bronchus at 5 min, 1, 6 and 12 h after antigen challenge. Each bar represents mean ± SE from 7 different animals.

to understand the beneficial effect of LLLT before LLLT can be used as a noninvasive therapy for the treatment of chronic asthma.

We have demonstrated that LLLT is an effective and beneficial treatment in relieving airway hyperresponsiveness by reducing the RhoA expression, and can reduce the calcium sensitivity in a model of acute lung inflammation induced by TNF (Aimbire et al., 2009; de Lima et al., 2010). In addition, acute lung inflammation is also influenced by LLLT, which down-regulates pro-inflammatory proteins and simultaneously up-regulates anti-inflammatory proteins, thereby promoting a counterbalance of Th1/Th2 cytokines, which controls the disease (de Lima et al., 2011a,b). On the basis of this finding, we proposed that LLLT could modulate bronchial hyperresponsiveness and lung inflammation in a rat allergic asthma model.

Our findings in the current study demonstrated that LLLT could modulate bronchial hyperresponsiveness via a mechanism independent of Ca^{+2} releases, which was potentially due to a G protein coupled receptor activation response. This was with the current study because LLLT attenuated BSM hyperresponsiveness due to a reduction in RhoA mRNA expression, which was attributed to MLC phosphatase inhibition. This inhibition resulted in the promotion of a contractile state, which was caused by Ca^{+2} sensitization of smooth muscle contraction. In addition, the late beneficial effect of laser, i.e., 24 h after last antigenic challenge was observed.

Thus, new therapies used to prevent an increase in RhoA protein expression in bronchial smooth muscle could modulate intracellular signaling, resulting in decreased hyperresponsiveness. Although the LLLT was efficient in reducing RhoA mRNA expression in BSM from antigen-challenged rats, we could not affirm that laser irradiation specifically affected RhoA protein expression at the membrane. Real Time-PCR was used in this study, which only detects mRNA expression. However, it is known that after translocation, RhoA protein is expressed at the BSM membrane. Thus, the effect of LLLT in reducing the RhoA mRNA expression in BSM is a strong indicator that the low-level laser is able to interfere with protein RhoA expression at the membrane.

In the present study, our results also suggested that LLLT could reduce inflammatory cell infiltration, increase BALF eosinophils and produced histological changes in lungs induced by antigen exposure, which were both attenuated by laser therapy. It is likely that the inhibitory effects of laser treatment on the inflammatory cell infiltration were due to an inhibition of pro-inflammatory cytokine release or IgE production because LLLT significantly altered the increased expression of IL-4, IL-5 and eotaxin in BAL after antigenic challenge.

Our results also suggested that the LLLT effect in reducing the bronchial hyperreactivity via RhoA was associated to its anti-inflammatory effect on IL-13 in BALF from allergic mice. It has been well established that levels of IL-13 were increased in bronchial lavage fluid of asthmatics, which induces specific significant features of bronchial asthma, including airway hyperresponsiveness (Horiba et al., 2011). Moreover, some studies have demonstrated a cross-talk between IL-13 and RhoA in the pulmonary system (Chiba et al., 2009). It was also been reported that IL-13 generated in the lung can induce an increase in RhoA expression in bronchial smooth muscle in asthmatic mice via STAT-6 (Goto et al., 2010). Thus, our findings suggested that the pronounced effect of the laser irradiation on bronchial hyperresponsiveness also reflects its action on the IL-13 pro-inflammatory cytokine. Moreover, it may also explain the marked laser anti-inflammatory effect on the number of eosinophils in BALF from asthmatic mice as an indirect response of the laser irradiation on IL-13. The laser effect on STAT6 reinforces the ability of this therapy to suppress the activity of the principal transcription factor involved in regulating IL-4, IL-5, IL-13 and eotaxin, which are pro-inflammatory mediators responsible by exacerbation and perpetuation of the allergic inflammatory response.

The total IgE in sera from antigen-challenged mice was not modified by LLLT. Since the first publication of the LLLT effect on acute airway and lung inflammation, we demonstrated that laser treatment did not present a systemic effect (Aimbire et al., 2005). In contrast, other studies have shown a LLLT systemic effect in different experimental models (Samoilova et al., 2008; Moreira et al., 2009). This negative result of the LLLT in the current study may be because the irradiation dose was too low to cause any significant change of IgE level in serum after antigen challenge or that the irradiated area was only surrounding the bronchi of the mice. However, local treatment with laser appeared to be advantageous because only the airway and lung was affected; thus, a potentially toxic effect of laser irradiation could be better controlled or even avoided. Our results reinforced the idea of using local treatment for allergic asthma.

Several studies have reported that STAT6 plays a pivotal role in the development of pulmonary eosinophilia, airway hyperresponsiveness and mucus hypersecretion (Hoshino et al., 2004). In the present study, we found that LLLT significantly reduced both the mRNA expression for STAT6 in lung tissue in animals challenged with antigen, and the concentration of cytokines, which function as chemoattractants for inflammatory cells, specifically eosinophils. On the basis of these results, it is reasonable to suggest that the anti-inflammatory effect of the laser irradiation on cytokines IL-4, IL-5, IL-13 and eotaxin in lung could be due to a reduction of STAT6 mRNA expression.

Some studies have demonstrated that the LLLT effect in vivo is not evidenced if the biological sample was analyzed just a few minutes after irradiation (Mafra de Lima et al., 2009a,b; de Lima et al., 2011a,b). Our results confirmed this observation. Although the interaction of the laser light with biological tissue occurred almost immediately, the laser effect at the cellular level required more time after the absorption of light by tissue to stimulate transcription factors to induce the generation or reduction of inflammatory proteins responsible for promoting the beneficial effect. Red or near infra-red laser fluencies as low as 3 or 5 J cm^{-2} will be beneficial in vivo, but large doses such as 50 or 100 J cm^{-2} will lose the beneficial effect and may even become detrimental (Chen et al., 2011).

It was observed in the present study that when laser irradiation was applied four times in a period of 24 h after antigenic challenged, a 5.4 J/cm^2 laser dose produced an in vivo beneficial effect on bronchial reactivity dysfunction and lung inflammation due to the reduction of pro-inflammatory cytokines release involved in lung allergic response. Accumulated laser doses in a short time period between the irradiations could cause some deleterious effect of LLLT or even eliminate its beneficial effect (Huang et al., 2009). To avoid this effect, the animals were irradiated four times at intervals

of 3 h from the first irradiation. Nevertheless, on the basis of these experiments, we could not establish the threshold dose capable of generating such a beneficial effect. However, the exposure time of the mice to laser irradiation clearly affected its inhibitory ability on airway hyperresponsiveness and lung inflammation, and thus could represent a target for future experiments.

5. Conclusions

The present study demonstrated for the first time that laser treatment relieves bronchial hyperresponsiveness via RhoA signaling and lung inflammation via STAT6 signaling in a mouse model of allergic asthma.

Acknowledgments

The present study was supported by a grant from Fundação de Amparo à Pesquisa do Estado de São Paulo (FAPESP) #. 2008/08838-5. We also would like to thank Eliane Gomes for the technical support.

References

Aimbire, F., Albertine, R., de Magalhães, R.G., Lopes-Martins, R.A., Castro-Faria-Neto, H.C., Zângaro, R.A., Chavantes, M.C., Pacheco, M.T., 2005. Effect of LLLT Ga–Al–As (685 nm) on LPS-induced inflammation of the airway and lung in the rat. Lasers Med. Sci. 20, 11–20.

Aimbire, F., de Lima, F.M., Costa, M.S., Albertini, R., Correa, J.C., Iversen, V.V., Bjordal, J.M., 2009. Effect of low-level laser therapy on bronchial hyper-responsiveness. Lasers Med. Sci. 24, 567–576.

Aimbire, F., de Oliveira, A.P.L., Albertini, R., Corrêa, J.C., de Campos, C.B.L., Lyon, J.P., Silva Jr., J.A., Costa, M.S., 2008. Low level laser therapy (LLLT) decreases pulmonary microvascular leakage, neutrophil influx and IL-1beta levels in airway and lung from rat subjected to LPS-induced inflammation. Inflammation 31, 189–197.

Akimoto, T., Numata, F., Tamura, M., Takata, Y., Higashida, N., Takashi, T., Takeda, K., Akira, S., 1998. Abrogation of bronchial eosinophilic inflammation and airway hyperreactivity in signal transducers and activators of transcription (STAT) 6-deficient mice. J Exp. Med. 187 (1998), 1537–1542.

Azzawi, M., Bradley, B., Jeffery, P.K., Frew, A.J., Wardlaw, A.J., Knowles, G., Assoufi, B., Collins, J.V., Durham, S., Kay, A.B., 1990. Identification of activated T lymphocytes and eosinophils in bronchial biopsies in stable atopic asthma. Am. Rev. Respir. Dis. 142, 1407–1413.

Barnes, P.J., 1999. Therapeutic strategies for allergic diseases. Nature 25, 31–38.

Bjordal, J.M., Johnson, M.I., Iversen, V.V., Aimbire, F., Lopes-Martins, R.A., 2006. Low-level laser therapy in acute pain: a systematic review of possible mechanisms of action and clinical effects in randomized placebo-controlled trials. Photomed. Laser Surg. 24, 158–168.

Boushey, H.A., Holtzman, M.J., Sheller, J.R., Nadel, A., 1980. Bronchial hyperreactivity. Am. Rev. Respir. Dis. 121, 389–413.

Broide, D.H., Gleich, G.J., Cuomo, A.J., Coburn, D.A., Federman, E.B., Schwartz, L.B., Wasserman, S.I., 1991. Evidence of ongoing mast cell and eosinophil degranulation in symptomatic asthma airway. J. Allergy Clin. Immunol. 188, 637–648.

Burney, P.G.J., 1997. In: Barnes, P.J., Grunstein, M.M., Leff, A.R., Woolcock, A.J. (Eds.), Epidemiologic Trends: Asthma. Lippincott Raven Inc., Philadelphia, pp. 281–304.

Busse, W.W., Lemanske, R.F., 2001. Asthma. N. Engl. J. Med. 344, 350–362.

Cayla, C., Merino, V.F., Cabrini, D.A., Silva Jr., J.A., Pesquero, J.B., Bader, M., 2002. Structure of the mammalian kinin receptor gene locus. Int. Immunopharmacol. 2, 1727–1730.

Chen, A.C., Arany, P.R., Huang, Y.Y., Tomkinson, E.M., Sharma, S.K., Arany, A.C., Kharkwal, G.B., Saleem, T., Mooney, D., Yull, F.E., Blackwell, T.S., Hamblin, M.R., 2011. Low-level laser therapy activates NF-kB via generation of reactive oxygen species in mouse embryonic fibroblasts. PLoS ONE 6, 22453–22456.

Chiba, Y., Sakai, H., Misawa, M., 2001. Augmented acetylcholine-induced translocation of RhoA in bronchial smooth muscle from antigen-induced airway hyperresponsiveness rats. Br. J. Pharmacol. 133, 886–890.

Chiba, Y., Sakai, H., Wachi, H., Sugitani, H., Seyama, Y., Misawa, M., 2003. Upregulation of RhoA mRNA in bronchial smooth muscle of antigen-induced airway hyperresponsiveness in rats. J. Smooth Muscle Res. 39, 221–228.

Chiba, Y., Sakai, H., Yu, Y., Misawa, M., 2005a. Effects of repeated antigen exposure on endothelin-1-induced bronchial smooth muscle contraction and activation of RhoA in sensitized rats. J. Biochem. 137, 751–756.

Chiba, Y., Ueno, A., Shinozaki, K., Takeyama, H., Nakazawa, S., Sakai, M.M., 2005b. Involvement of RhoA-mediated Ca^{2+} sensitization in antigen-induced bronchial smooth muscle hyperresponsiveness in mice. Respir. Res. 6, 4–7.

Chiba, Y., Nakazawa, S., Todoroki, M., Shinozaki, K., Sakai, H., Misawa, M., 2009. Interleukin-13 augments bronchial smooth muscle contractility with an up-regulation of RhoA protein. Am. J. Respir. Cell. Mol. Biol. 40, 159–167.

Chow, R.T., Heller, G.Z., Barnsley, L., 2006. The effect of 300 mW, 830 nm laser on chronic neck pain: a double-blind, randomized, placebo-controlled study. Pain 124, 201–210.

Chow, R.T., Johnson, M.I., Lopes-Martins, R.A., Bjordal, J.M., 2009. Efficacy of low-level laser therapy in the management of neck pain: a systematic review and meta-analysis of randomized placebo or active-treatment controlled trials. Lancet 374, 1897–1908.

de Lima, F.M., Bjordal, J.M., Albertini, R., Santos, F.V., Aimbire, F., 2010. Low-level laser therapy (LLLT) attenuates RhoA mRNA expression in the rat bronchi smooth muscle exposed to tumor necrosis factor-alpha. Lasers Med. Sci. 25, 661–668.

de Lima, F.M., Moreira, L.M., Villaverde, A.B., Albertini, R., Castro-Faria-Neto, H.C., Aimbire, F., 2011a. Low-level laser therapy (LLLT) acts as cAMP-elevating agent in acute respiratory distress syndrome. Lasers Med. Sci. 26, 389–400.

de Lima, F.M., Villaverde, A.B., Albertini, R., Corrêa, J.C., Carvalho, R.L., Munin, E., Araújo, T., Silva Jr., J.A., Aimbire, F., 2011b. Dual Effect of low-level laser therapy (LLLT) on the acute lung inflammation induced by intestinal ischemia and reperfusion: action on anti- and pro-inflammatory cytokines. Lasers Surg. Med. 43, 410–420.

Emson, C.L., Bell, S.E., Jones, A., Wisden, W., McKenzie, A.N., 1998. Interleukin (IL)-4-independent induction of immunoglobulin (Ig) E, and perturbation of T cell development in transgenic mice expressing IL-13. J. Exp. Med. 188, 399–404.

Esaulenko, I.E., Nikitin, A.V., Shatalova, O.L., 2009. The use of laserpuncture in patients with asthma bronchial and concomitant rhinosinusitis. Vopr. Kurortol. Fizioter. Lech. Fiz. Kult. 1, 37–39.

Farkhudtinov, U.R., 2007. Intravascular laser irradiation of blood in the patients with bronchial asthma. Ter. Arkh. 79, 44–48.

Gosens, R., Schaafsma, D., Nelemans, S., Halayko, A.J., 2006. Rho-kinase as a drug target for the treatment of airway hyperresponsiveness in asthma. Mini Rev. Med. Chem. 6, 339–348.

Goto, K., Chiba, Y., Matsusue, K., Hattori, Y., Maitani, Y., Sakai, H., Kimura, S., Misawa, M., 2010. The proximal STAT6 and NF-kappaB sites are responsible for IL-13- and TNF-alpha-induced RhoA transcriptions in human bronchial smooth muscle cells. Pharmacol. Res. 61, 466–472.

Horiba, M., Qutna, N., Gendapodi, P., Agrawal, S., Sapkota, K., Abel, P., Townley, R.G., 2011. Effect of IL-1β and TNF-α vs IL-13 on bronchial hyperresponsiveness, β2-adrenergic responses and cellularity of bronchial alveolar lavage fluid. Auton. Autacoid Pharmacol. 31, 37–49.

Hoshino, A., Tsuji, T., Matsuzaki, J., Jinushi, T., Ashino, S., Teramura, T., Chamoto, K., Tanaka, Y., Asakura, Y., Sakurai, T., Mita, Y., Takaoka, A., Nakaike, S., Takeshima, T., Ikeda, H., Nishimura, T., 2004. STAT6-mediated signaling in Th2-dependent allergic asthma: critical role for the development of eosinophilia, airway hyper-responsiveness and mucus hypersecretion, distinct from its role in Th2 differentiation. Int. Immunol. 16, 1497–1505.

Huang, Y.Y., Chen, J.D., Carroll, M.R., Hamblin, M.R., 2009. Biphasic dose response in low level light therapy. Dose Response 7, 358–383.

Jeffery, P.K., 1993. Microscopic structure of airway secretory cells: variation in hypersecretory disease and effects of drugs. In: Takishima, T., Shimura, S. (Eds.), Airway Secretion: Physiological Basis for the Control of Mucus Hypersecretion. Marcel Dekker, Inc., New York, pp. 149–215.

Kaplan, M.H., Schindler, U., Smiley, S.T., Grusby, M.J., 1996. Stat6 is required for mediating responses to IL-4 and for development of Th2 cells. Immunity 4, 313–319.

Kashanskaia, E.P., Fedorov, A.A., 2009. Low-intensity laser radiation in the combined treatment of patients with chronic obstructive bronchitis. Vopr. Kurortol. Fizioter. Lech. Fiz. Kult. 2, 19–22.

Kuperman, D., Schofield, B., Wills-Karp Grusby, M.J., 1998. Signal transducer and activator of transcription factor 6 (Stat6)-deficient mice are protected from antigen-induced airway hyperresponsiveness and mucus production. J. Exp. Med. 187, 939–948.

Lampl, Y., Zivin, J.A., Fisher, M., Lew, R., Welin, L., Dahlof, B., Borenstein, P., Andersson, B., Perez, J., Caparo, C., Ilic, S., Oron, U., 2007. Infrared laser therapy for ischemic stroke: a new treatment strategy: results of the NeuroThera Effectiveness and Safety Trial-1 (NEST-1). Stroke 38, 1843–1849.

Landyshev, Iu.S., LAvdeeva, N.V., Goborov, N.D., Krasavina, N.P., Tikhonova, G.A., Tkacheva, S.I., 2002. Efficacy of low intensity laser irradiation and sodium nedocromil in the complex treatment of patients with bronchial asthma. Ter. Arkh. 74, 25–28.

Livak, F., Fourigny, M., Schatz, D., 1999. Characterization of TCR gene rearrangements during adult murine T cell development. J. Immunol. 162, 2575–2580.

Louis, R., Schleich, F., Barnes, P.J., 2012. Corticosteroids: still at the frontline in asthma treatment? Clin. Chest Med. 33, 531–541.

Mafra de Lima, F., Costa, M.S., Albertini, R., Silva Jr., J.A., Aimbire, F., 2009a. Low level laser therapy (LLLT): attenuation of cholinergic hyperreactivity, β(2)-adrenergic hyporresponsiveness and TNF-alpha mRNA expression in rat bronchi segments in *E. coli* lipopolysaccharide-induced airway inflammation by a NF-kappaB dependent mechanism. Lasers Surg. Med. 41, 68–74.

Mafra de Lima, F., Naves, K.T., Machado, A.H., Albertini, R., Villaverde, A.B., Aimbire, F., 2009b. Lung inflammation and endothelial cell damage are decreased after treatment with phototherapy (PhT) in a model of acute lung injury induced by *Escherichia coli* lipopolysaccharide in the rat. Cell. Biol. Int. 33, 1212–1221.

Martin, J.G., Duguet, A., Eidelman, D.H., 2000. The contribution of airway smooth muscle to airway narrowing and airway hyperresponsiveness in disease. Eur. Respir. J. 16, 349–354.

Milojevic, M., Kuruc, V., 2003. Low power laser biostimulation in the treatment of bronchial asthma. Med. Pregl. 56, 413–418.

Moreira, M.S., Velasco, I.T., Ferreira, L.S., Ariga, S.H., Barbeiro, D.F., Meneguzzo, D.T., Abatepaulo, F., Marques, M.M., 2009. Effect of phototherapy with low intensity laser on local and systemic immunomodulation following focal brain damage in rat. J. Photochem. Photobiol. B 97, 145–151.

Nedeljković, M., Ljustina-Pribić, R., Savić, K., 2008. Innovative approach to laser acupuncture therapy of acute obstruction in asthmatic children. Med. Pregl. 61, 123–130.

Nikitin, A.V., Eusalenko, I.E., Shatalova, O.L., 2008. Effectiveness of laser puncture in elderly patients with bronchial asthma. Vopr. Kurortol. Lech. Fiz. Kult. 6, 38–39.

Ohashi, Y., Motojima, S., Fukuda, T., Makino, S., 1992. Airway hyperresponsiveness, increased intracellular spaces of bronchial epithelium, and increased infiltration of eosinophils and lymphocytes in bronchial mucosa in asthma. Am. Rev. Respir. Dis. 145, 1469–1476.

Ostronosova, N., 2006. Outpatient use of laser therapy in bronchial asthma. Ter. Arkh. 78, 41–44.

Pires, D., Xavier, M., Araújo, T., Silva Jr., J.A., Aimbire, F., Albertini, R., 2011. Low-level laser therapy (LLLT; 780 nm) acts differently on mRNA expression of anti- and pro-inflammatory mediators in an experimental model of collagenase-induced tendinitis in rat. Lasers Med. Sci. 26, 85–94.

Samoilova, K.A., Zhevago, N.A., Petrishchev, N.N., Zimin, A.A., 2008. Role of nitric oxide in the visible light-induced rapid increase of human skin microcirculation at the local and systemic levels: II. Healthy volunteers. Photomed. Laser Surg. 26, 443–449.

Seow, C.Y., Schellenberg, R.R., Paré, P.D., 1998. Structural and functional changes in the airway smooth muscle of asthmatic subjects. Am. J. Respir. Crit. Care Med. 158, 179–186.

Takeda, K., Tanaka, T., Shi, W., Matsumoto, M., Minami, M., Kashiwamura, S., Nakanishi, K., Yoshida, N., Kishimoto, T., Akira, S., 1996. Essential role of Stat6 in IL-4 signaling. Nature 380, 627–630.

Virchow, J.C., Barnes, P.J., 2012. Asthma Semin. Respir. Crit. Care Med. 33, 577–585.

Wiggs, B.R., Moreno, R., Hogg, J.C., Hilliam, C., Paré, P.D., 1990. A model of the mechanics of airway narrowing. J. Appl. Physiol. 69, 849–860.